J Physiol (2003), **549.3**, *pp.* 809–821

DOI: 10.1113/jphysiol.2002.033290
www.jphysiol.org

Journal of Physiology

Orexins induce increased excitability and synchronisation of rat sympathetic preganglionic neurones

Marco van den Top, Matthew F. Nolan*, Kevin Lee, Peter J. Richardson†, Ruud M. Buijs‡, Ceri H. Davies§ and David Spanswick

*Department of Biological Sciences, The University of Warwick, Coventry CV4 7AL, UK, *Centre for Neurobiology and Behavior, Columbia University, 1051 Riverside Drive, NY 10032 USA, †Department of Pharmacology, University of Cambridge, Tennis Court Road, Cambridge CB2 1QJ, UK, ‡Netherlands Institute for Brain Research, Meibergdreef 33, Amsterdam, 1105 AZ, The Netherlands and §GlaxoSmithKline Pharmaceuticals, Coldharbour Road, The Pinnack, Harlow, Essex CM19 5AD, UK*

The neuropeptides orexin A and B are synthesised by perifornical and lateral hypothalamic (LH) neurones and exert a profound influence on autonomic sympathetic processes. LH neurones project to spinal areas containing sympathetic preganglionic neurones (SPNs) and therefore may directly modulate sympathetic output. In the present study we examined the possibility that orexinergic inputs from the LH influence SPN activity. Orexin-positive neurones in the LH were labelled with pseudorabies virus injected into the liver of parasympathetically denervated animals and orexin fibres were found adjacent to the soma and dendrites of SPNs. Orexin A or B (10–1000 nM) directly and reversibly depolarised SPNs in spinal cord slices. The response to orexin A was significantly reduced in the presence of the orexin receptor 1 (OX1R) antagonist SB334867A at concentrations of 1–10 μM. Single cell reverse transcriptase-polymerase chain reaction revealed expression of mRNA for both OX1R and OX2R in the majority of orexin-sensitive SPNs. The orexin-induced depolarisation involved activation of pertussis toxin-sensitive G-proteins and closure of a K^+ conductance via a protein kinase A (PKA)-dependent pathway that did not require an increase in intracellular Ca^{2+}. Orexins also induced biphasic subthreshold membrane potential oscillations and synchronised activity between pairs of electrically coupled SPNs. Coupling coefficients and estimated junctional conductances between SPNs were not altered indicating synchronisation is due to activation of previously silent coupled neurones rather than modulation of gap junctions. These findings are consistent with a direct excitation and synchronisation of SPNs by orexinergic neurones that *in vivo* could increase the frequency and coherence of sympathetic nerve discharges and mediate LH effects on sympathetic components of energy homeostasis and cardiovascular control.

(Received 29 September 2002; accepted after revision 20 March 2003; first published online 17 April 2003)
Corresponding author D. Spanswick: Department of Biological Sciences, University of Warwick, Coventry CV4 7AL, UK.
Email: dspanswick@bio.warwick.ac.uk

Orexin A and B (hypocretin A and B) are recently identified neuropeptides derived from the precursor protein prepro-orexin (or prepro-hypocretin), which, in the central nervous system, is expressed exclusively by a subset of neurones within and around the perifornical nucleus and lateral hypothalamus (LH; de Lecea *et al.* 1998; Sakurai *et al.* 1998). Centrally and spinally administered orexins increase heart rate, arterial pressure and sympathetic activity (Samson *et al.* 1999; Shirasaka *et al.* 1999; Chen *et al.* 2000; Artunes *et al.* 2001; Matsumura *et al.* 2001). The release of orexins may therefore contribute to LH effects on sympathetic output which are important for the cardiovascular components of defensive responses (Smith *et al.* 1990; Ledoux, 1995) and for the control of body weight and energy homeostasis (Bernardis & Bellinger, 1993). In addition, dense orexinergic projections innervate the intermediolateral cell column (IML) of the spinal cord (van den Pol, 1999; Date *et al.* 2000), where the majority of sympathetic preganglionic neurone (SPN) cell bodies reside (Coote, 1988), suggesting LH orexinergic neurones may act directly on SPNs.

An improved understanding of the function of orexins requires knowledge of their receptor expression and cellular actions in anatomically identified target neurones. In the present study we addressed the hypothesis that LH orexinergic neurones directly modulate the output of SPNs and explored the cellular mechanisms involved. We have examined the anatomical relationship between orexinergic neurones and central neural pathways

M. van den Top and M. F. Nolan contributed equally to this work.

influencing sympathetic output and investigated the actions of orexins on the electrophysiological properties of SPNs in spinal cord slices. A preliminary account of these findings has appeared in abstract form (van den Top *et al.* 2000).

METHODS

Immunohistochemistry

For a detailed description of immunohistochemical and pseudorabies virus (PRV) tracing methods see Buijs *et al.* (2001). All PRV studies were carried out at the Netherlands Institute for Brain Research. Briefly, adult male Wistar rats were anaesthetised with sodium pentobarbital (25 mg kg^{-1}, I.P.), and ketamine hydrochloride (70 mg kg^{-1}, I.P.) and 2 μl of PRV-Bartha containing 1×10^8 plaque-forming units was injected into the liver. Immediately afterwards, the parasympathetic innervation of the liver was cut leaving the sympathetic supply intact. The hepatic parasympathectomy was performed as follows. A laparotomy was performed in the midline, and the fascia containing the hepatic branch was stretched by gently moving the stomach and the oesophagus. With a myelin-specific dye (Toluidin Blue) the hepatic branch could be revealed as it separates from the left vagal trunk. With the aid of a binocular operating microscope (× 10–25 magnification), the stained neural tissue was transected between the ventral vagus trunk and the liver. Small blue-stained branches running in the fascia between the stomach and the liver were transected. Rats were completely hepatic parasympathetic denervated as evidenced by the complete absence of staining in the dorsal motor nucleus of the vagus or nucleus ambiguus. Particular care was taken not to damage the dorsal and the ventral trunks innervating the stomach and abdominal tissues and the blood vessels that run along the hepatic vagus branches. Animals were allowed to recover, then after 2 or 3 days were killed under deep anaesthesia with sodium pentobarbital (100 mg kg^{-1}, I.P.), and perfused through the left ventricle with saline, followed by a solution of 4 % paraformaldehyde and 0.15 % glutaraldehyde in phosphate-buffered saline.

Brains and spinal cord were removed, kept overnight in 4 % paraformaldehyde in phosphate-buffered saline, cryoprotected by immersion in 30 % sucrose in 0.2 M phosphate buffer for a further 72 h, then frozen on dry ice and coronal sections were cut using a cryostat. Sections were washed in 0.05 M Tris-buffered saline and incubated overnight at 4 °C with antibody specific for orexin A (1:10 000; Peptide Institute, Osaka, Japan). The sections were washed then incubated in secondary antibody conjugated to CY5. Sections were subsequently incubated with a monoclonal mouse anti-PRV antibody (1:10 000), washed and incubated with a secondary antibody conjugated to fluorescein isothiocyanate (FITC). Sections were viewed with a confocal laser scanning microscope.

Electrophysiology

Male Sprague-Dawley or Wistar rats, aged 10–21 days, were deeply anaesthetised with enflurane or halothane (7 % in O_2; Abbott laboratories, Kent, UK) and killed by decapitation. The spinal cord was rapidly removed and transverse 300–400 μm slices cut using a Vibratome (Intracel, Series 1000, Royston, UK). Slices were maintained at room temperature in oxygenated artificial cerebrospinal fluid (ACSF) for at least 1 h prior to recording. For recording, slices were continuously perfused with ACSF (flow 3–8 ml min^{-1}, temperature 33 ± 1 °C). The composition of the ACSF was (mM): 127.0 NaCl, 1.9 KCl, 1.2 KH_2PO_4, 26.0 $NaHCO_3$, 10.0 D-glucose, 1.3 $MgCl_2$ and 2.4 $CaCl_2$, equilibriated with 95 % O_2, 5 % CO_2, pH 7.3–7.4. The following channel blockers were added to the ACSF where stated: 0.5–1 μM tetrodotoxin (TTX) to block voltage-gated Na^+ channels; 0.1 mM carbenoxolone to block gap junction-mediated electrical synaptic transmission; 1–2 mM Cs^+ or 0.1 mM Ba^{2+} to block fast inward rectification. ACSF containing 16 mM K^+ was prepared by replacing equimolar amounts of NaCl with KCl. Reduced K^+ ACSF was prepared by substitution of Na^+ salts for K^+ salts.

Recordings were obtained from neurones located in the IML of the spinal cord using axopatch-1D amplifiers (Axon Instruments, Foster City, CA, USA). Patch pipettes were pulled using a horizontal puller (Sutter Instrument Co, Novato, CA, USA) from thin-walled borosilicate glass capillaries (Clarke Electromedical) and had resistances between 4 and 7 MΩ when filled with recording solution. The whole-cell pipette solution comprised (mM): 120 potassium gluconate, 10 NaCl, 2 $MgCl_2$, 0.5 K_2EGTA, 10 Hepes, 4 Na_2ATP and 0.3 Na_2GTP, pH 7.2, whilst for perforated patch-clamp recordings it comprised (mM): 140 potassium gluconate, 10 Hepes, 1 EGTA and 10 KCl, with 250 μg ml^{-1} amphotericin-B and 5 μg ml^{-1} gramicidin, pH 7.2.

Whole-cell recordings were performed under visual control using infrared video microscopy (Stuart *et al.* 1993). Perforated-patch recordings were performed using methods described in detail previously (van den Top *et al.* 2001). Appropriate series resistance compensation was performed and recordings were terminated when series resistances changed by more than 15 %. Cells were identified as SPNs based on their location and characteristic electrophysiological properties (Pickering *et al.* 1991; Logan *et al.* 1996). Current and voltage data were displayed on-line on a digital oscilloscope (Gould DSO1602), filtered at 2–5 kHz and 1 kHz, respectively and stored on DAT (Biological DTR-1205, Intracel). For data analysis the signal was digitized at 2–10 kHz, stored on a personal computer running pClamp7 and analysed using Axograph 3 software (Axon Instruments) run on a Macintosh Power PC. In current-clamp experiments, cells were maintained at their resting potential. Input resistance was determined from the steady-state membrane potential response to small (< 40 pA) current steps. To evaluate orexin-induced changes in input resistance, membrane potential during application of orexin was adjusted to the pre-orexin baseline by injecting constant current. Constant amplitude current pulses were superimposed on the background current. The coupling coefficient and junctional conductance were determined during paired recordings as described previously (Nolan *et al.* 1999). In voltage-clamp experiments neurones were held at −60 mV, the series resistance was compensated by 60–80 % and current signals were filtered at 1 kHz using a 4-pole low-pass Bessel filter.

Drugs used were orexin A and B (from Bachem, St Helens, UK), BAPTA, carbenoxolone, pertussis toxin (PTX), adenosine 3′,5′-cyclic monophosphorothioate (Rp-cAMPS), thapsigargin and 1-(6–9[(17β)-3-methoxyestra-1,3,5(10)-trien-17-yl]amino-hexyl]-1*H*-pyrrole-2,5-dione (U73122) (all from Sigma), tetrodotoxin (from Alomone Labs, Jerusalem, Israel) and (1-(2-methylbenzoxazol-6-yl)-3-[1,5]napthyridin-4-yl-urea hydrochloride (SB334867A; a gift from GlaxoSmithKline). BAPTA, thapsigargin, SB334867A and U73122 were initially dissolved in 100 % DMSO and then diluted in ACSF or intracellular solution resulting in a maximal concentration of 0.5 % DMSO. Stock solutions of the other drugs were made in distilled water and diluted in ACSF. All drugs were bath applied from reservoirs connected to the ACSF

flow line by manually operable three-way valves. Agonists were applied in 10 ml boluses, antagonists and blockers were perfused for at least 10 min before examining their effects on agonist responses.

Single cell reverse transcriptase-polymerase chain reaction (RT-PCR)

For single cell RT-PCR the cytosolic contents of SPNs shown to be sensitive to orexins using whole-cell recording techniques were aspirated into the recording pipette under visual control. The contents of the electrode were forced into a microtube and the RNA reverse transcribed using an anchored oligo dT primer and 200 units of Moloney murine leukaemia virus (MMLV) reverse transcriptase (BRL) according to the manufacturer's recommendations. After 60 mins at 37 °C the cDNA was stored frozen at −20 °C prior to processing. After amplification of the cDNA using Taq polymerase in a 3′-end amplification (TPEA) PCR, the expression of specific genes was measured using primers designed to amplify products of between 150 and 250 base pairs in length, close to the 3′ ends of the mRNA transcripts (Dixon *et al.* 1998; Lee *et al.* 1999).

The primers used were: for OX1R (GenBank accession number AF041244), forward primer (bases 2196–2213): CAGGCATATCCACCTGGC; reverse primer (bases 2333–2315): ACACCTGGAGAGGGTGGAC; OX2R (accession number AF041246), forward primer (bases 2620–2643): ACATCCTCTCCATCATTTTATGCA; reverse primer (bases 2754–2733): AGTTGGGGGAGTCTTCTGTCCC; α-tubulin (accession number V01226); forward primer (bases 298–316): CACTGGTACGTGGGTGAGG; reverse primer (bases 469–448): TTTGACATGATACAGGGACTGC; ribosomal protein L11 (accession number X62146); forward primer (bases 405–425): TTCTATGTGGTGCTGGGTAGG; reverse primer (bases 504–485): TTGCCTCCTCTTTGCTGATT; β-actin (accession number V01217); forward primer (bases 3527–3544): CATCCATGCCCTGAGTCC; reverse primer (bases 3736–3717): ACACCTCAAACCACTCCCAG. These PCR reactions were run for 40 cycles of 92 °C (denaturing, 2.5 min), 55 °C (annealing, 1.5 min) and 72 °C (extension, 1 min), followed by a final extension of 10 min at 72 °C. The PCR products were separated on 2.5 % agarose gels and the product sizes were as predicted from the sequences. In control experiments on diluted brain cDNA, all primer pairs were able to detect positive products of the predicted size using 0.1 pg of cDNA but not 0.01 pg. Furthermore, in experiments where the electrode was positioned next to a cell without seal formation or harvesting of the cytoplasmic contents, no PCR products were detected ($n = 3$).

Statistical analyses

All values are expressed as the mean ± S.E.M. Student's two-tailed t test was used for all statistical analysis in the paired and independent configuration as appropriate. All statistical analyses were performed on a PC running Microsoft Excel.

RESULTS

Sympathetic projections of orexin neurones

We first asked whether orexin-containing neurones are part of the central network controlling sympathetic output. PRV injected into peripheral organs is transported along neuronal processes and passes trans-synaptically from post- to presynaptic neurones enabling it to be used to label multisynaptic pathways controlling sympathetic output (Strack *et al.* 1989; Strack & Loewy, 1990). Central pathways influencing the sympathetic supply to the liver were labelled by PRV injected into the liver of animals that were parasympathetically denervated. SPNs were labelled by PRV 2 days after the injection (Fig. 1*Ai* and *Aii*) while LH neurones were labelled after 3 days (Fig. 1*B*). The presence of orexin-containing neurones was determined by double-labelling of sections with antibodies against orexin A. In spinal sections (levels T5–T10) orexin-positive fibres were labelled adjacent to the soma and dendrites of PRV-positive SPNs (Fig. 1*Ai* and *Aii*). In the LH, a subpopulation of orexin-positive neurones was double-labelled with PRV. In LH sections from three animals, a total of 423 orexin-positive cell bodies were detected, of which 41 were double-labelled with PRV, and 382 were PRV negative. In addition, 96 PRV-labelled orexin-negative neurones were also found in the LH suggesting neurones other than orexin-containing neurones innervate SPNs (Fig. 1*B*). These findings indicate that a subpopulation of orexinergic neurones in the LH contribute to central

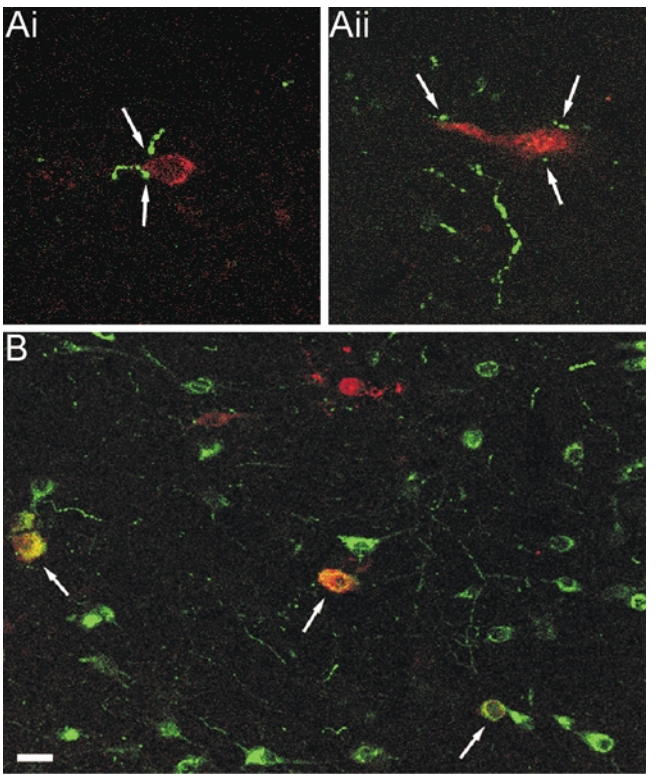

Figure 1. Confocal laser scanning micrographs of transverse sections of spinal cord and hypothalamus

Sections were labelled for PRV (red) and orexin A (green). PRV was injected into the liver of parasympathetically denervated animals and retrogradely transported via the sympathetic nervous system to the central nervous system. *Ai* and *Aii*, Two PRV-labelled SPNs stained red, 2 days after injection, in close contact with orexin fibres stained green (arrows). *B*, PRV-labelled LH neurons, 3 days after virus injection, indicating the presence of neurones involved in the sympathetic control of the liver. Orexin-positive neurones were also present in the LH with approximately 10 % co-localised (yellow) with PRV (arrows). Scale bar shown in *B* corresponds to 10 μm in *A* and 25 μm in *B*.

pathways influencing sympathetic output to the liver, and synapse directly with SPNs.

Orexins depolarise SPNs

We next investigated the actions of orexins on the membrane properties of SPNs using perforated patch-clamp recordings. Bath application of 100 nM orexin A induced membrane depolarisations from an average resting membrane potential of −61.0 ± 1.9 mV to −51.5 ± 2.3 mV. Thus orexin A induced a reversible depolarisation of 9.5 ± 1.6 mV (Fig. 2*A*; $n = 13$). This depolarisation was maintained in the presence of 500 nM TTX (10.5 ± 2.6 mV; Fig. 2*B*; $n = 11$) and was concentration dependent in nature (Fig. 2*C*). Perfusion of orexin A in the presence of TTX induced a 7.7 ± 0.9, 17.5 ± 2.3 and 22.0 ± 1.8 mV depolarisation at concentrations of 10, 100 and 1000 nM, respectively (Fig. 2*C*; data from four neurones). Orexin B also caused a reversible, concentration-dependent depolarisation of SPNs that was maintained in the presence of TTX. No significant difference was found between depolarising responses to 100 nM orexin A and 100 nM orexin B compared in three SPNs (orexin A, 7.9 ± 0.5 mV; orexin B, 9.5 ± 0.8 mV; $P = 0.15$; Fig. 2*A*; $n = 3$). Orexin A and B induced similar responses when recordings were made in the whole-cell configuration, which was subsequently used for single cell RT-PCR experiments, investigation of second messenger pathways and dual recordings. All other data were obtained with perforated patch-clamp recordings. Orexin A was used in all subsequent experiments described here.

To clarify the nature of the receptors mediating orexin-induced responses, the effects of the selective OX1R antagonist SB334867A were investigated. Orexin A-induced responses were maintained upon repeated application (up to five consecutive responses, $n = 12$) of the agonist to the same cell (Fig. 3*A*). The orexin receptor antagonist SB334867A (1–10 μM) (Smart *et al.* 2001; Soffin *et al.* 2002) reduced responses to orexin A ($n = 6$, Fig. 3*B*). The reduction of the orexin A response by SB334867A was similar with an antagonist concentration of 1 or 10 μM, thus the data were pooled (Fig. 3*C*). The orexin A-induced depolarisation was significantly reduced from a peak amplitude of 14.5 ± 2.3 mV in control to

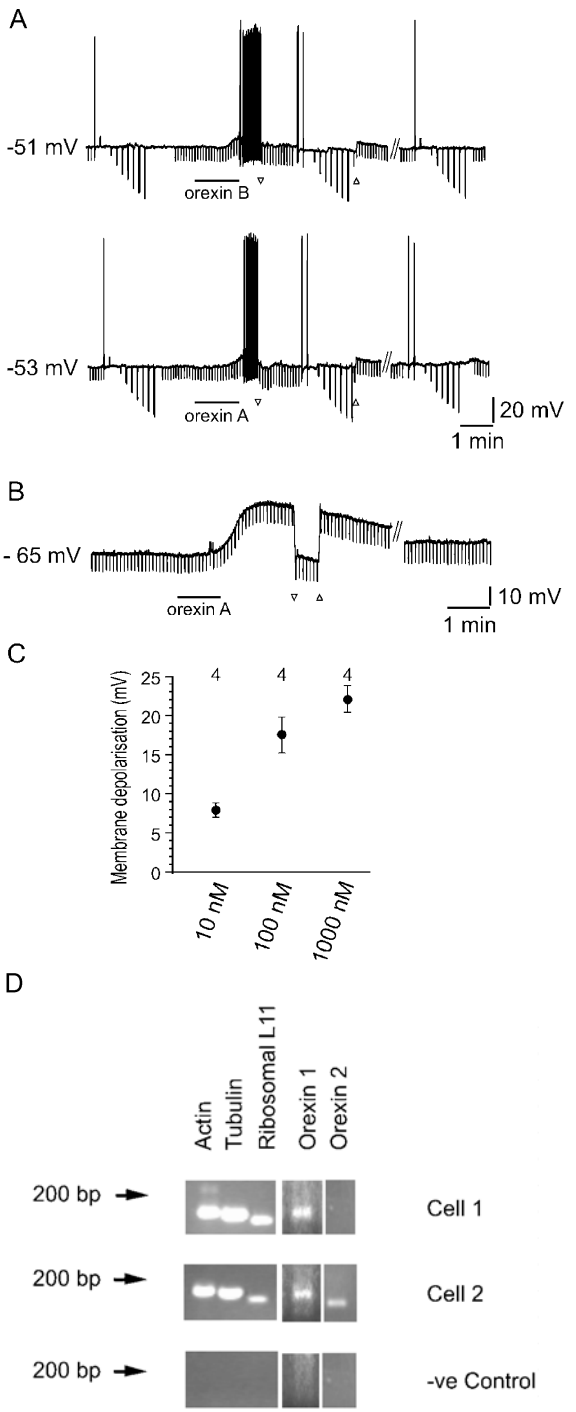

Figure 2. SPNs express orexin receptors and are directly depolarised by orexins

A, 100 nM orexin B (top) or 100 nM orexin A (bottom) induce a reversible depolarisation of the same SPN. ▽ and △ indicate the start and end, respectively, of constant negative current injection to reveal the increase in input resistance. The duration of the orexin application is indicated by the bar under the trace. // indicates a break in the trace of 15 min. *B*, the orexin A response was maintained in the presence of 500 nM TTX indicating it was acting directly on SPNs. As in *A*, ▽ and △ denote the start and end, respectively, of constant negative current injection and the bar under the trace indicates 100 nM orexin A application. // indicates a break in the trace of 15 min. *C*, plot of the concentration dependence of orexin-induced membrane depolarisation in SPNs. Circles and error bars indicate the mean and S.E.M., respectively. Data are from 4 cells. *D*, single cell RT-PCR of mRNA extracted from orexin A-responsive SPNs showed the presence of mRNA for OXR1 only (top) or OXR1 and OXR2 (bottom) in addition to housekeeper genes actin, tubulin and ribosomal L11 as positive controls. The negative (−ve) control was performed on the contents of an electrode placed next to a cell without seal formation or harvesting of the cytoplasmic contents.

5.9 ± 1.8 mV in the presence of SB334867A ($n = 6$; $P < 0.05$). These data suggest that SPNs express functional orexin receptors 1 and 2.

To determine whether SPNs express orexin receptor mRNA, single cell RT-PCR was performed from orexin-sensitive SPNs. To control for variations in cytoplasmic sampling efficiency, only those cells that expressed the housekeeping genes actin, tubulin and ribosomal protein L11 were tested for OX1R and OX2R mRNA. All of the sampled cells expressing mRNA for orexin receptors were depolarised by orexin A. In the first series of experiments, the presence of mRNAs encoding OX1R and OX2R was shown in 7/8 (87.5 %) and 2/8 (25 %) neurones, respectively (Fig. 2*D*). Increasing the sensitivity of detection by using more of the TPEA product in the gene-specific PCR reaction (Surmeier *et al.* 1996) increased the number of cells detected that expressed OX2R (67 %, 4/6), but not OX1R (83.3 %, 5/6), indicating that OX2R mRNA is at levels close to the limit of detection in most cells.

Thus the pharmacological properties of orexin responses and pattern of orexin receptor expression indicate that orexin receptors 1 and 2 are expressed by SPNs and their activation causes membrane depolarisation. However, in the absence of selective pharmacological tools their relative contribution to orexin responses remains unclear.

Mechanisms underlying the orexin-induced depolarization

The mechanisms mediating the depolarisation of SPNs by orexin A were investigated further. The orexin A-induced depolarisation was associated with a reversible increase in input resistance (Fig. 2*A* and *B*) in 17 of 18 SPNs. In response to perfusion of 100 nM orexin A, input resistance increased from 469 ± 93 to 610 ± 131 MΩ ($n = 10$, $P < 0.05$) and returned to 473 ± 96 MΩ after washout of orexin from the bath. Furthermore orexin A (100 nM), in the presence of TTX, increased input resistance in 8 of 11 SPNs tested from 437 ± 67 to 518 ± 83 MΩ (Fig. 2*B*; $n = 8$; $P < 0.05$), indicating that the decreased membrane conductance is due to a direct effect on SPNs.

Current–voltage relationships were obtained from nine SPNs in control conditions and at the peak of the orexin-induced depolarisation. In three of the nine cells tested the orexin-induced conductance change had a reversal potential of −91.3 ± 3.8 mV, close to the reversal potential for K^+ ions of −101 mV under our recording conditions, indicating closure of K^+ channels (Fig. 4*A* and *B*). In the remaining cells, the difference between control and orexin current–voltage relationships decreased at potentials approaching −90 mV, however no clear reversal potential was observed. In cells not exhibiting a clear reversal potential, replacing extracellular K^+ with Na^+ to make the K^+ reversal more negative, increased the magnitude of the orexin-induced depolarisation ($n = 2$; Fig. 4*C*). Conversely, shifting the K^+ reversal in a positive direction by increasing extracellular K^+ to 16 mM attenuated orexin responses ($n = 3$).

The lack of clear reversal potential may be due to a contribution to the orexin response of poorly space-clamped channels at locations electrically distant from the soma, for example on distal dendrites or on adjoining SPNs connected by electrical synapses (see also Travagli *et al.* 1995). The anomalous inward rectifying current would exaggerate this problem by increasing shunting of distal

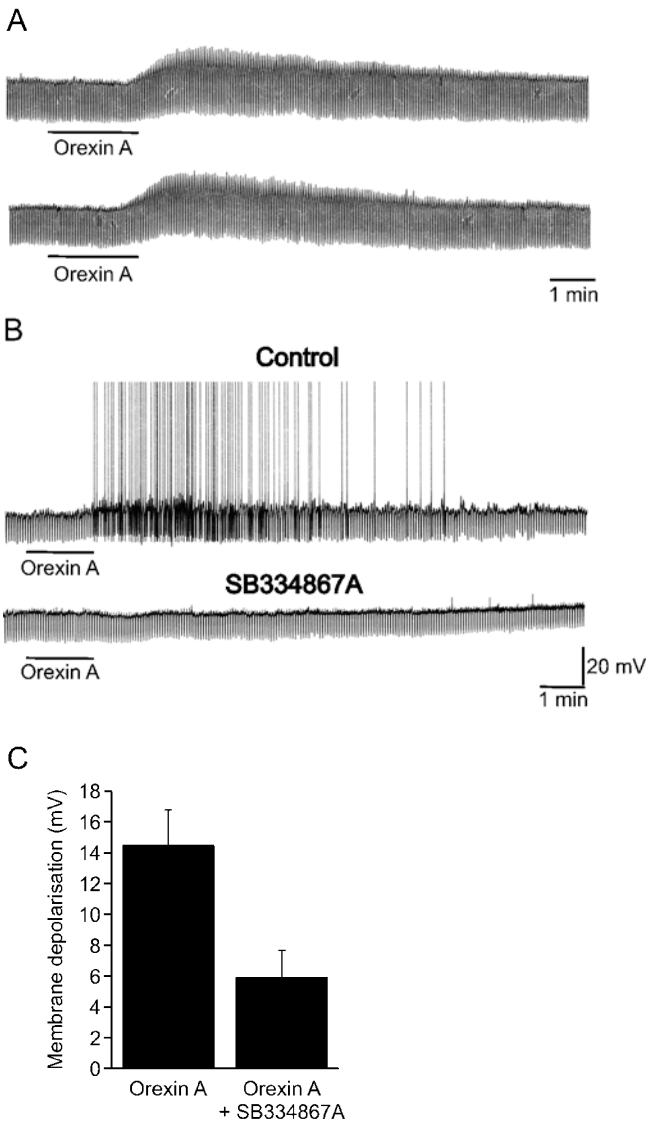

Figure 3. Orexin-induced depolarisation is reduced by the OX1R anatagonist SB334867A

A, samples of a continuous whole-cell recording showing orexin A-induced reversible depolarisations in SPN that were not subject to desensitisation. *B*, orexin A induced a membrane depolarisation sufficient to reach threshold for firing in another SPN, an effect that was subsequently reduced following exposure of the slice to SB334867A (1 μM). *C*, summary histogram of pooled orexin-induced depolarisations in the presence and absence of SB334867A (1–10 μM). The error bars represent the S.E.M.

conductances at potentials close to the K^+ reversal potential. We attempted to obtain more reliable estimates of the reversal potential for orexin-induced excitation by uncoupling SPNs with the gap-junction blocker carbenoxolone (100 μM, $n = 5$), blocking Na^+ channels with TTX and blocking the anomalous inward rectification with Cs^+ (1–2 mM, $n = 2$, Fig. 4*D*) or Ba^{2+} (100 μM, $n = 3$). Under these conditions, orexin induced an inward current of mean peak amplitude 10 ± 3 pA ($n = 5$) in cells voltage clamped at −60 mV. Voltage ramps from −120 mV to −20 mV at a rate of 10 mV s^{-1} revealed the inward current was associated with a decrease in input conductance. Superimposition of voltage ramps prior to and during application of orexin again failed to reveal a clear reversal

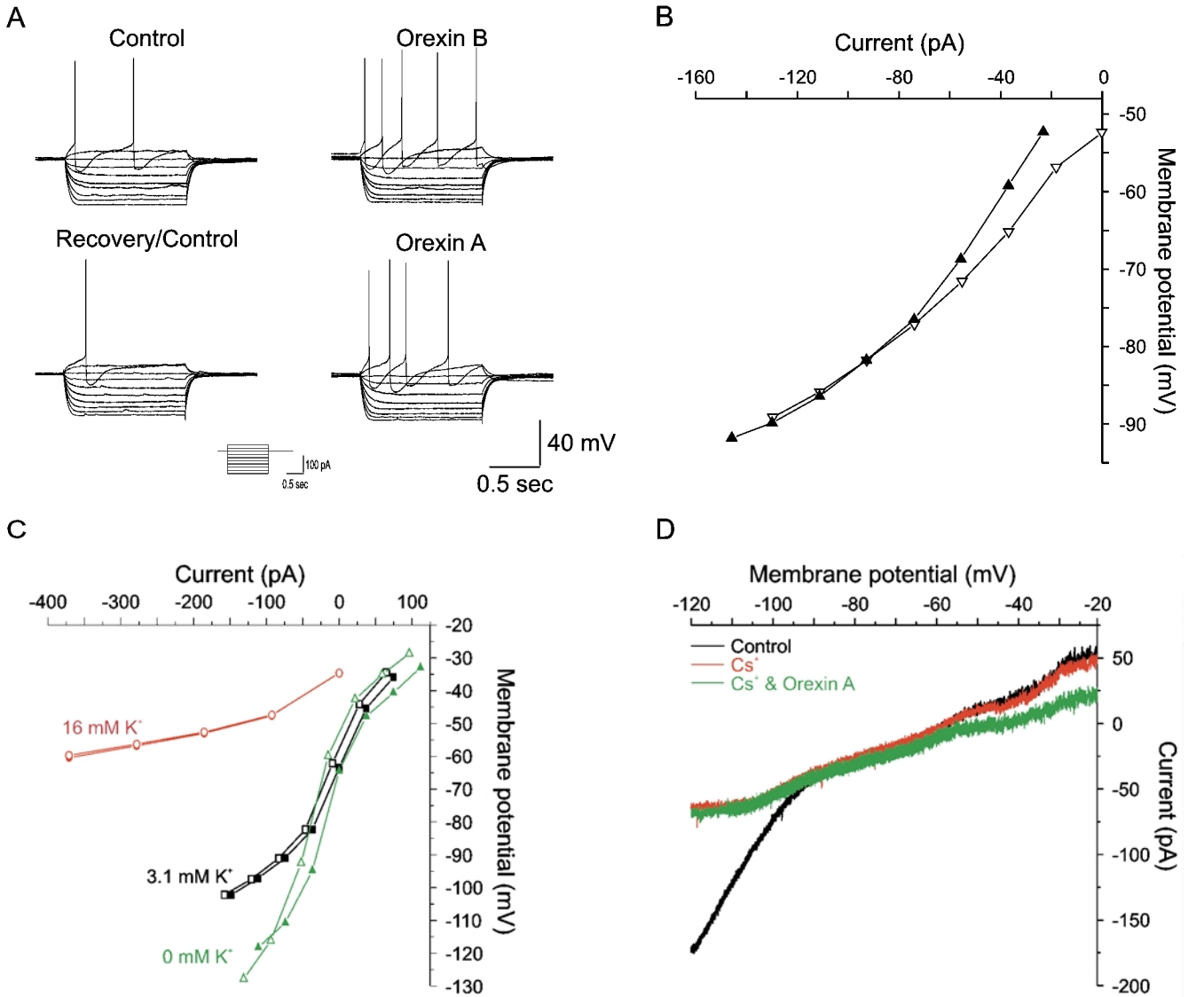

Figure 4. Effects of orexins on the current–voltage relationships of SPNs

A, membrane potential responses of an SPN to a series of current steps (inset) before (upper and lower left) and during perfusion of orexin A (lower right) and orexin B (upper right). *B*, plot of the current–voltage relationships for the traces in *A*. Orexin A (▽, control; ▲, orexin) increased the slope of the *I–V* relationship indicating closure of channels with a reversal potential of approximately −82 mV. Similar data were obtained with orexin B (not shown). *C*, in a different neurone an increase (●, control; ○, orexin) and decrease (▲, control; △, orexin) in the extracellular potassium concentration from the control concentration (■, control; □, orexin) results in shifts in the extrapolated reversal potentials. Furthermore, a reduction and increase in extracellular K^+ concentration resulted in a decrease and increase in the amplitude of the orexin A-induced depolarisation, respectively. *D*, voltage-clamp recordings from a SPN showing the current response to voltage ramps from −120 to −20 mV (10 mV s^{-1}) in the presence of TTX (0.5 μM) and the gap-junction blocker carbenoxolone (100 μM). Perfusion of Cs^+ (1 mM) blocked the anomalous inward rectification. In the presence of TTX, carbenoxolone and Cs^+ the orexin response attenuated with increasing hyperpolarisation, however no obvious reversal potential was indicated.

potential for the orexin-induced response (Fig. 4*D*). These data are consistent with the block of a resting potassium conductance contributing to the orexin-induced membrane depolarisation, although modulation of additional membrane conductances or pumps may also occur.

To determine whether the orexin-induced depolarisation requires activation of G-proteins we examined the effect of pre-treating slices with PTX. Alternate slices from the same animal were incubated for 18–36 h in either control ACSF or ACSF containing 4 μg ml^{-1} PTX. Whole-cell recordings were made alternately from PTX-treated and control slices and responses to perfusion of 500 nM orexin A were examined (Fig. 5*A*). Orexin A-induced depolarisations were significantly reduced in PTX-treated slices (Fig. 5*B*; control 9.8 ± 2.6 mV, $n = 8$; PTX 1.7 ± 1.2 mV, $n = 12$, $P < 0.01$), indicating that the orexin-induced depolarisation involves activation of PTX-sensitive G-proteins.

We next examined the possible involvement of intracellular Ca^{2+} signalling in the orexin-induced depolarisation. The EGTA in the standard intracellular solution was replaced with 10 mM BAPTA to increase the buffering of intracellular Ca^{2+}. Under these conditions, the magnitude of the depolarisation induced by orexin A was not significantly different from the depolarisation observed in the absence of BAPTA (control, 12.5 ± 2.6 mV; 10 mM BAPTA 14.1 ± 1.3 mV; $P = 0.68$; $n = 3$; Fig. 5*B*). Furthermore, inhibition of phospholipase C (PLC) via pre-incubation with 10 μM U73122 (Bleasdale *et al.* 1990) or depletion of intracellular calcium stores by bath application of thapsigargin had no effect on the amplitude of depolarisation induced by 100 nM orexin A ($P = 0.26$ and 0.27, respectively; $n = 3$; Fig. 5*B*).

To investigate the role of cAMP/PKA signalling, the effects of inhibiting cAMP with Rp-cAMPS (10 μM, $n = 4$) were tested on orexin-induced responses. Bath application of Rp-cAMPS alone induced a membrane depolarisation of 3.8 + 1.5 mV. Rp-cAMPS therefore partially mimicked the response to orexin. Subsequent exposure to orexin in the presence of Rp-cAMPS significantly attenuated the magnitude of the depolarisation induced by 100 nM orexin A (control, 14.8 ± 4.8 mV; 10 μM Rp-cAMPS, 6.5 ± 2.2 mV; $n = 4$; $P < 0.05$; Fig. 5*B*).

Subthreshold oscillations and synchronisation induced by orexins

In a subpopulation of silent SPNs, subthreshold oscillations in membrane potential, with a biphasic waveform consisting of a rapid depolarisation followed by a more prolonged hyperpolarising component occur in response to neurotransmitter agonists (Pickering *et al.* 1994; Gibson & Logan, 1995; Spanswick *et al.* 1995; Nolan & Logan, 1998). The oscillations arise from passive conduction via electrical synapses of action potentials from adjoining neurones and do not involve chemical synaptic interactions or intrinsic spiking (Spanswick & Logan, 1990; Logan *et al.* 1996; Nolan *et al.* 1999). Perfusion of 100 nM orexin A induced biphasic membrane potential oscillations in 4 of 15 silent SPNs in which oscillations were not previously observed. The time course of the orexin-induced oscillatory response was similar to that of the membrane depolarisation (Fig. 6*A* and *B*). In the remaining 11 silent neurones orexin-induced membrane depolarisation was not associated with the induction of oscillations, presumably reflecting a lack of electrotonic coupling in these SPNs. A

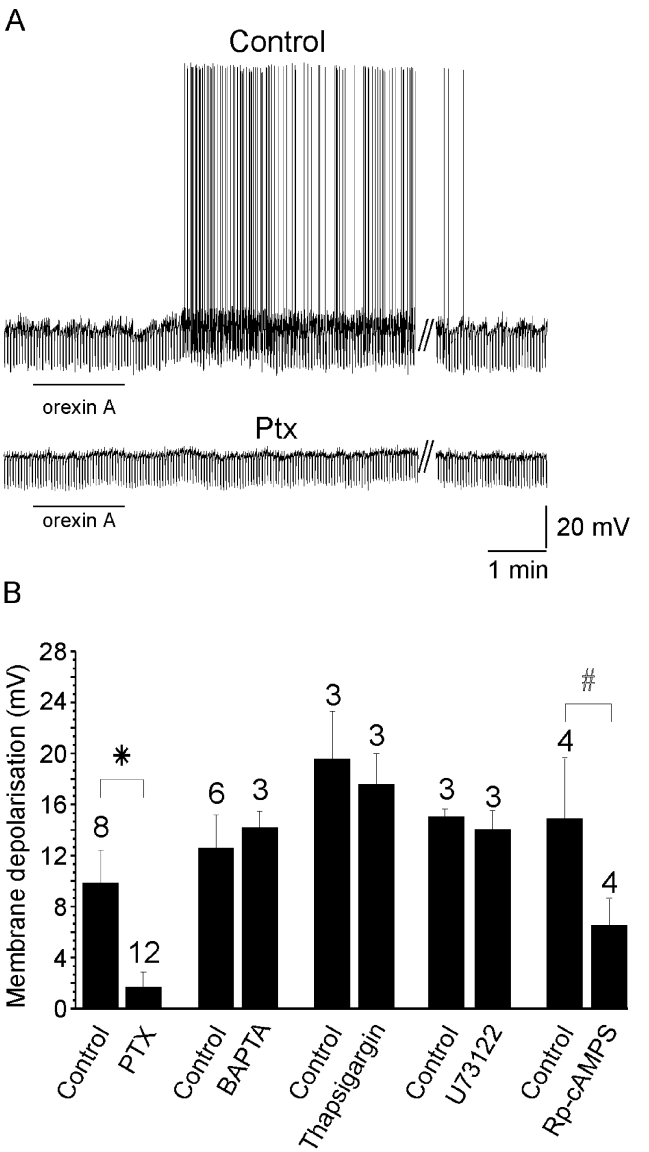

Figure 5. Orexin-induced depolarisation involves a PTX-sensitive G-protein and PKA signalling

A, orexin-induced depolarisation from a control experiment and from a PTX-treated slice. The line under the trace indicates the application of orexin A while // indicates a 15 min washout period. *B*, summary histogram of pooled orexin-induced depolarisation for PTX, BAPTA, thapsigargin, U73122 and Rp-cAMPS. The error bars represent the S.E.M. The numbers above the bars indicate the number of experiments. * $P < 0.01$, #$P < 0.05$.

second subpopulation of SPNs is characterised by spontaneous ongoing membrane potential oscillations which are due to spontaneous spiking in adjoining electrically coupled, spontaneously spiking SPNs (Spanswick & Logan, 1990; Logan *et al.* 1996). Perfusion of orexin A caused an increase in the amplitude and frequency of oscillations in four of five of these cells. In the other cell a decrease in the amplitude and frequency of spontaneous biphasic oscillations was observed in the presence of orexin.

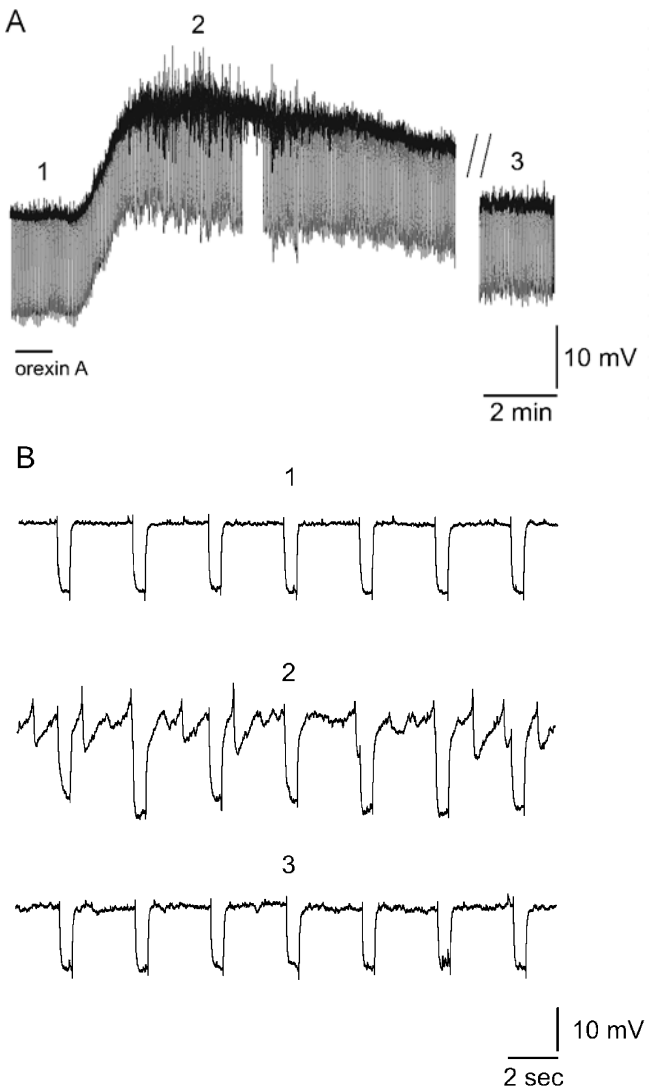

Figure 6. Orexin-induced oscillations in SPNs

A, current-clamp recording of orexin A-induced biphasic membrane potential oscillations in a previously silent SPN. The onset and duration of the period of oscillatory activity is similar to that of the orexin-induced depolarisation. Orexin A (100 nM) application is marked by a line under the trace. // represents a break in the trace of duration 10 min. The numbers above the trace mark the regions shown on an expended time scale in *B*. *B*, expanded time scale of the trace in *A* illustrating the membrane potential oscillations which are characterised by a rapid depolarisation followed by a slower more prolonged hyperpolarisation. The regular, rectangular waveform, negative membrane potential deflections in *A* and *B* are responses to injection of negative current steps in order to monitor the input resistance of the neurone.

Subthreshold membrane potential oscillations may serve as a mechanism for the synchronisation of activity between SPNs connected by electrical synapses (Spanswick & Logan, 1990; Logan *et al.* 1996; Nolan *et al.* 1999). We therefore tested whether orexin induction of biphasic oscillations and action potentials in previously silent neurones is synchronised between neurons, by recording simultaneously from pairs of SPNs. Electrical synaptic connections between SPNs were demonstrated by injection of current steps into either neurone and observation of a corresponding membrane polarisation in the adjoining neurone. Orexin A-induced biphasic membrane potential oscillations and action potentials occurred synchronously in the two neurones in all pairs of previously silent, electrically coupled SPNs examined ($n = 3$; Fig. 7*A*). In contrast, orexin A did not induce synchronous activity between pairs of neurones that were not demonstrated to be directly coupled to one another ($n = 3$; Fig. 7*B*i and *B*ii). Thus, orexins appear to be able to induce synchronous activity only in SPNs that are already electrically coupled to one another.

The induction of synchronous oscillations in silent SPNs may be due to the modulation of existing electrical synapses rather than the opening of new synaptic connections. We therefore examined the effects of orexin A on the properties of electrical synapses between pairs of SPNs. Orexin was applied to three pairs of electrically coupled SPNs in control ACSF and three pairs of electrically coupled SPNs in the presence of ACSF containing TTX. In all six pairs examined, electrical coupling was bi-directional and voltage independent before and during perfusion of orexin A (Fig. 8*A*, *B* and *C*). Coupling coefficients were similar before and during perfusion of 100 nM orexin A (control 0.28 ± 0.03, orexin A 0.29 ± 0.04, $P = 0.67$). The mean estimated coupling conductance was also similar before and during perfusion of 100 nM orexin A (control 1.62 ± 0.44 nS, orexin A 1.43 ± 0.32 nS, $P = 0.28$). In addition, orexin A did not induce coupling between non-coupled pairs of SPNs ($n = 3$; Fig. 8*D*). Thus, orexins do not appear to modulate gap-junction coupling between SPNs, but instead induce oscillations and synchronisation by suprathreshold depolarisation of networks of previously silent SPNs connected by existing electrical synapses.

DISCUSSION

The present study supports the hypothesis that LH orexinergic neurones have direct excitatory actions on SPNs via activation of orexin receptors. Orexin-positive neurones in the LH were labelled by PRV transported from the liver of parasympathetically denervated animals and

orexin-containing fibres were found adjacent to the cell bodies and dendrites of SPNs. Orexin A and B directly depolarised SPNs, responses that were in part reduced by the OX1R antagonist SB334867A, and mRNAs for OX1R and OX2R were expressed by these neurones. The intracellular signalling pathway activated by orexins involved PTX-sensitive G-proteins and the PKA-dependent closure of an unidentified resting K^+ conductance. Taken together these data indicate SPNs express functional OX1 and OX2 receptors. In networks of electrically coupled SPNs, orexins induced subthreshold membrane potential oscillations and synchronous activity. This did not require a change in the strength of electrical coupling, but rather was due to simultaneous depolarisation of coupled SPNs.

The data described provide evidence that LH orexinergic neurones influence sympathetic output to the liver by direct actions on SPNs. Previous studies have demonstrated orexin-positive fibres in the IML of the spinal cord (van den Pol, 1999; Date *et al.* 2000) and orexin-positive neurones in the LH that project to SPNs that target the pancreas (Buijs *et al.* 2001). In the present study PRV injected into the liver of parasympathetically denervated rats labelled a subpopulation of orexin-positive neurones in the LH, indicating functional division of orexin neurons, with the PRV-positive population able to directly influence sympathetic output to the liver. Labelling of orexin-positive LH neurones by PRV within 3 days of peripheral injection indicates these are second order neurones that synapse directly onto SPNs (Buijs *et al.* 2001). In agreement with this, we also demonstrated orexin fibres adjacent to the soma and dendrites of labelled SPNs, expression of orexin receptor mRNA by SPNs and direct depolarisation of SPNs by orexins. The majority of SPNs at all spinal levels were sensitive to orexins indicating that sympathetic targets other than the liver are influenced by orexin inputs to SPNs. As central expression of orexins is exclusively by neurones in the region of the LH, SPN orexin receptors are only likely to decode inputs from LH neurones. However, we cannot rule out additional influences of orexinergic neurones on sympathetic output by actions on neurones projecting to SPNs, for example via the rostral ventrolateral medulla (Chen *et al.* 2000) or via actions on spinal interneurones. Furthermore, as we have not demonstrated a direct synaptic response mediated by orexin, we cannot discount the possibility that the effects of orexin observed reflected activation of functional non-synaptic receptors that act to sense circulating levels of orexin.

Orexins A and B at concentrations of 10–1000 nM depolarised SPNs. In agreement with the findings of Artunes *et al.* (2001), comparison of the mean responses to

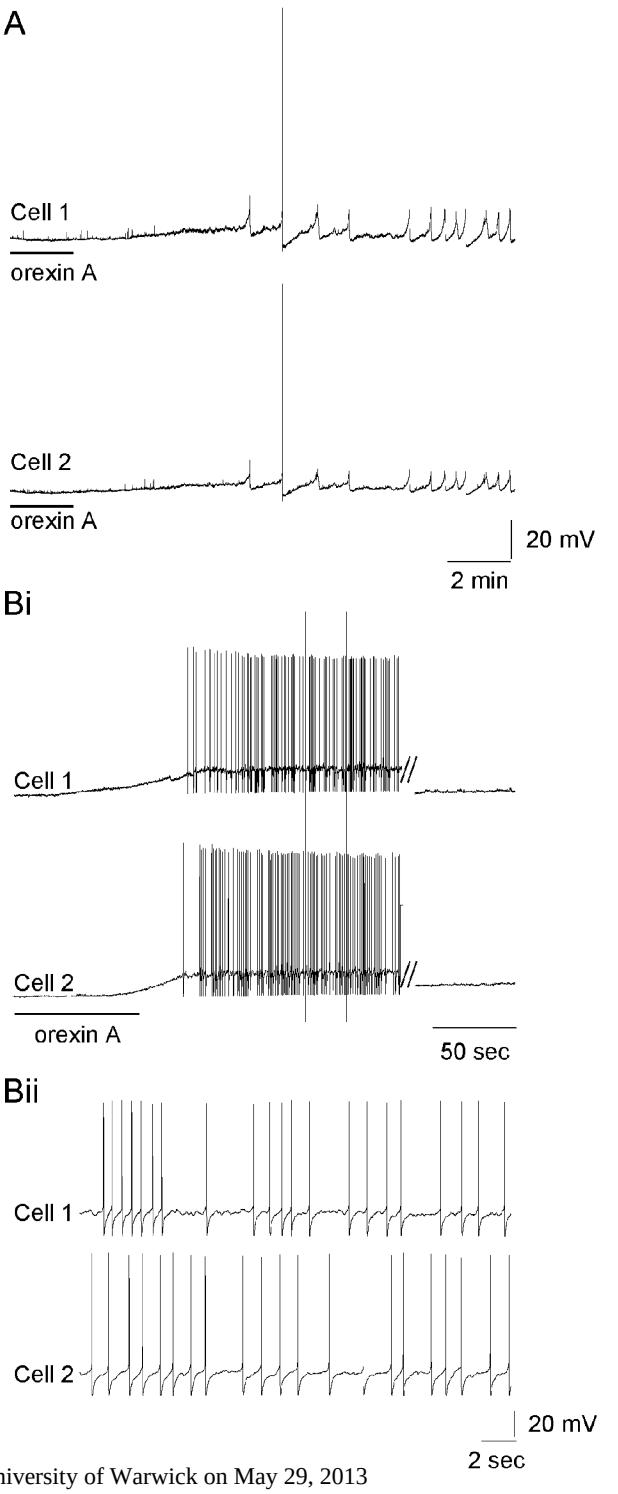

Figure 7. Orexin-induced synchronous activity in electrically coupled SPNs

A, simultaneous recording from two electrically coupled SPNs reveals the induction of synchronised activity following orexin A (500 nM) application. Biphasic membrane potential oscillations and action potential firing are synchronised between the two SPNs. *Bi*, simultaneous recording of two SPNs that are not electrically connected to each other. Orexin application induces asynchronous action potential firing and membrane oscillations in both neurones. // indicates a 15 min break in the presented recording. *Bii*, expanded trace from *Bi* demonstrating the asynchronous action potential firing of non-coupled SPNs.

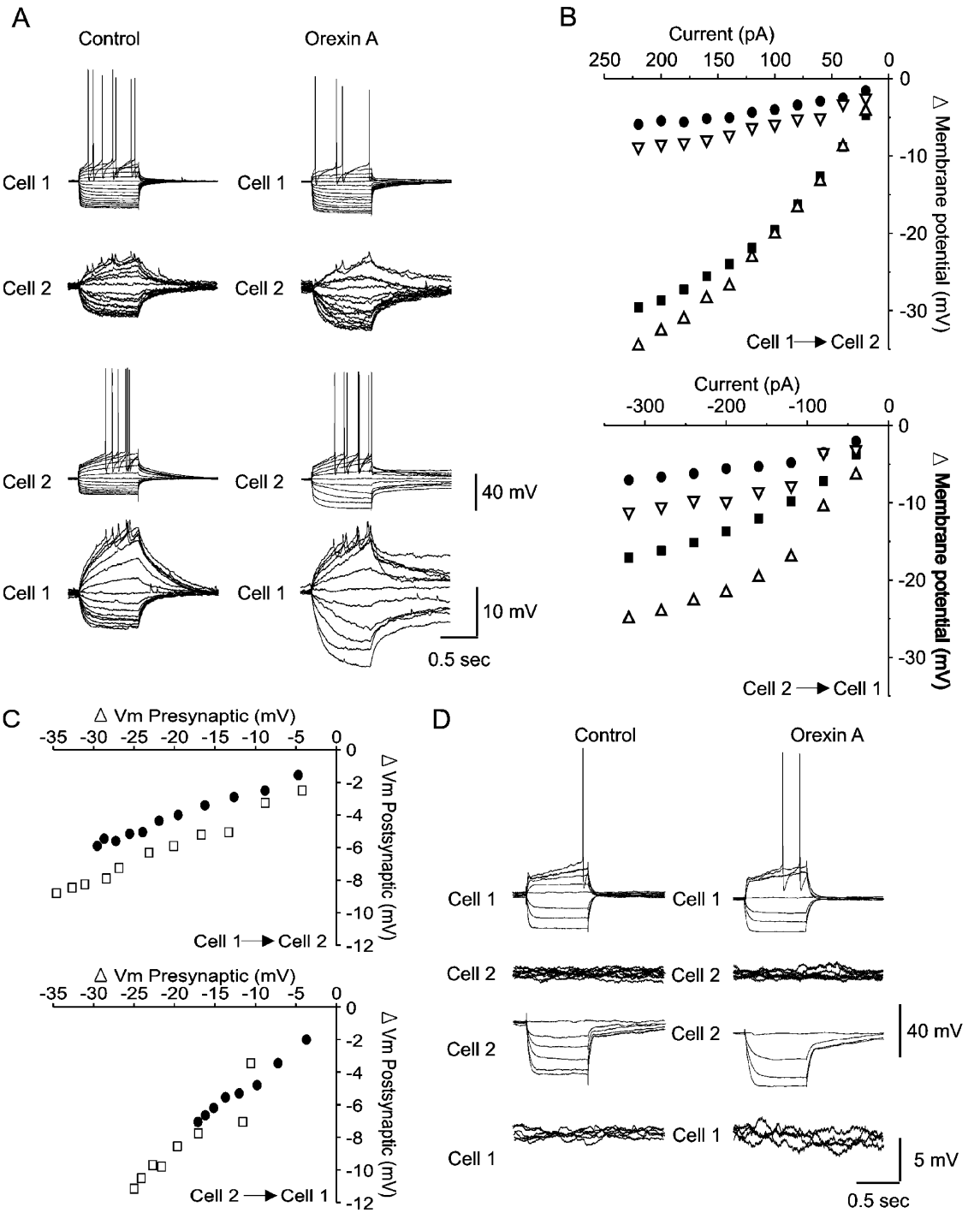

Figure 8. Orexin A induces oscillations without modifying electrical synapses between SPNs

A, *I–V* relationships obtained from an electrically coupled pair of SPNs before and during 400 nM orexin A-induced depolarisation. Current steps injected into cell 1 result in a membrane response in both cell 1 and cell 2 (top). The electrical synapses are bi-directional allowing similar current transfer from cell 2 to cell 1 following current injection in cell 2 (bottom). *B*, plot of the relationship between the injected current and the steady-state membrane potential change in the absence and presence of orexin for current injection in cell 1 (top) and cell 2 (bottom). The plots reveal a linear relationship between the size of the current step and the resulting membrane response in the injected and the non-injected cell. Explanation of symbols: ■, control injected; ●, control non-injected; △, orexin injected ; ▽, orexin non-injected. *C*, plot of the relationship between pre- and postsynaptic changes in membrane potential between cell 1 and cell 2 (top) and cell 2 and cell 1 (bottom) in the absence (●) and presence (□) of orexin. *D*, *I–V* relationships illustrating lack of current transfer in non-coupled SPNs. Current injection in cell 1 results in no membrane response in cell 2 (left) and similarly, current transfer from cell 2 to cell 1 does not occur. Orexin does not induce electrical coupling in either direction (right).

orexin A and B did not reveal significant differences in the potency of the two agonists. This is consistent with activation of OX2R which has similar sensitivity to orexins A and B, unlike OX1R which has approximately 20-fold higher affinity for orexin A (Sakurai *et al.* 1998, 2000). However, responses to orexin A were sensitive to the selective OX1R antagonist SB334867A, being reduced by over 50 % in the presence of this agent, and single cell RT-PCR analysis indicated that OX2R and OX1R were expressed in the majority of SPNs. Taken together these data suggest SPNs express both functional OX1 and OX2 receptors. Further clarification of orexin receptor subtypes mediating the observed excitation of SPNs, and their differential expression and role in regulating SPN excitability will require the use of further selective pharmacological agents or genetic tools and immunohistochemistry with selective antibodies.

A combination of current- and voltage-clamp experiments were used to investigate the ionic mechanism of the orexin-induced depolarisation. The depolarisation was associated with an increase in input resistance and in three neurones had a reversal potential close to the K^+ reversal potential, indicating that closure of a K^+ conductance contributes to the depolarisation. However, in many SPNs, the orexin response was reduced by hyperpolarisation towards the K^+ reversal potential, but did not reverse. In these cells, manipulations of extracellular K^+ concentration altered the response in a manner consistent with the involvement of a K^+ conductance. The absence of a clear reversal potential did not appear to be due to a contribution of currents at electrically distant and therefore poorly space-clamped locations, as after uncoupling SPNs with carbenoxolone and blocking inward rectification with Ba^{2+} or Cs^+, we were still unable to obtain reliable reversal potentials. Under these conditions, orexin-induced currents approached zero at potentials negative to the K^+ reversal potential, indicating that a Ba^{2+}- and Cs^+-insensitive K^+ conductance contributes to the inward current and membrane depolarisation. The failure to obtain an accurate reversal potential may be due to the voltage dependence of the potassium channels. However, it is also possible that additional ion channels or pumps may contribute to the orexin-induced depolarisation. In relation to this, previous studies in other central nervous system areas have revealed orexin to regulate neuronal excitability via a number of different mechanisms. For example, locus coerulus neurones, which contain mRNA for OX1R, were also depolarised by orexin A by a mechanism that suggested closure of potassium channels (Hagan *et al.* 1999; Horvath *et al.* 1999; Ivanov & Aston-Jones, 2000; Soffin *et al.* 2002). However, in immature LC neurons, orexin depolarisations appear to be mediated by a TTX-insensitive Na^+ current (van den Pol *et al.* 2002). Orexin A also depolarises serotonergic neurones from the dorsal raphe nucleus, which contains mRNA for OX1R and OX2R (Brown *et al.* 2001), and in cultured hypothalamic neurones expressing OX1R and OX2R, orexin elevates intracellular calcium and enhances synaptic currents (van den Pol *et al.* 1998).

The sensitivity of the orexin responses to PTX indicates that they are mediated by activation of either Gi or Go. Go activation is typically linked to stimulation of PLC with subsequent changes in intracellular Ca^{2+} levels whilst Gi is usually linked to inhibition of cAMP signalling. Our results suggest that a Go-mediated mechanism is unlikely to be involved in the response described here since PLC inhibition by U73122, intracellular Ca^{2+} buffering with 10 mM BAPTA and Ca^{2+} store depletion with thapsigargin all failed to modify the orexin response. In contrast, PKA inhibition with Rp-cAMPS both mimicked the response to orexin and reduced the magnitude of the orexin-mediated depolarisation suggesting that a Gi-mediated inhibition of cAMP is likely to contribute to the observed depolarisation.

Synchronised biphasic membrane potential oscillations and action potentials were induced by orexins during recordings from pairs of electrically coupled SPNs, but not SPNs that did not show evidence of electrical coupling. Thus, *in vivo* orexins may not only increase the frequency of sympathetic discharges, but may also induce synchronous discharges from coupled SPNs which would increase the coherence of sympathetic nerve activity and the probability that preganglionic firing will discharge post-ganglionic neurones. Coupling coefficients and estimated coupling conductance between pairs of SPNs were not altered by orexins, indicating that orexins do not directly modulate gap junction coupling between SPNs. Rather, the observed oscillations may simply be due to suprathreshold depolarisation of adjoining electrically coupled SPNs. A similar increase in oscillations and synchronous activity has been reported in immature LC neurones (van den Pol *et al.* 2002) which are also electrically coupled (Travagli *et al.* 1995); however, the effects of orexins on gap junction coupling were not examined.

Neurones in the LH are involved in the control of feeding/energy metabolism and also mediate autonomic responses to defensive behaviour. Activation of orexinergic neurones following fasting is indicated by changes in c-Fos expression (Lin & Huang, 1999). One consequence of such activation may be to increase the activity of SPNs innervating the liver and pancreas, which would cause physiological changes associated with glucose mobilisation such as gluconeogenesis and reduced insulin secretion. It is also possible that orexins contribute to autonomic components of defensive behaviours mediated via the LH, for example in response to stimuli used for fear conditioning (LeDoux, 1995). Centrally administered orexins have cardiovascular effects including elevation of blood pressure and heart rate (Shirasaka *et al.* 1999; Chen *et al.* 2000; Artunes *et al.* 2001) which are similar to the cardiovascular components of responses initiated from the LH (Smith *et al.* 1990).

Orexinergic neurones may also influence other regions involved in autonomic control including the locus coeruleus (de Lecea *et al.* 1998), nucleus of the solitary tract (Sunter *et al.* 2001), raphe nuclei (Greco & Shiromani, 2001) and parasympathetic areas in the spinal cord (Date *et al.* 2000). It is likely therefore that their activation causes a co-ordinated change in the activity of central autonomic networks.

In conclusion, the present study shows a direct excitatory effect of orexin on SPNs via the closure of one or more potassium conductances that normally contribute to the resting membrane potential. Future clarification of the role of orexins in sympathetic control *in vivo* will require spatially restricted pharmacological manipulations to localise the site of orexin actions and selective antagonists to distinguish their contribution to basal tone and reflex/conditional changes in sympathetic output.

REFERENCES

Artunes VR, Brailoiu GC, Kwok EH, Scruggs P& Dun NJ (2001). Orexins/hypocretins excite rat sympathetic preganglionic neurons *in vivo* and *in vitro*. *Am J Physiol* **281**, R1801–1807.

Bernardis LL& Bellinger LL (1993). The lateral hypothalamic area revisited – neuroanatomy, body-weight regulation, neuroendocrinology and metabolism. *Neurosci Biobehav Rev* **17**, 141–193.

Bleasdale JE, Thakur NR, Gremban RS, Bundy GL, Fitzpatrick FA, Smith RJ & Bunting S (1990). Selective inhibition of receptor-coupled phospholipase C-dependent processes in human platelets and polymorphonuclear neutrophils. *J Pharm Exp Ther* **256**, 756–768.

Brown RE, Sergeeva O, Eriksson KS & Haas H (2001). Orexin A excites serotonergic neurons in the dorsal raphe nucleus of the rat. *Neuropharmacology* **40**, 457–459.

Buijs RM, Chun SJ, Niijima A, Romijn HJ & Nagai K (2001). Parasympathetic and sympathetic control of the pancreas, a role for the suprachiasmatic nucleus and other hypothalamic centers that are involved in the regulation of food intake. *J Comp Neurol* **431**, 405–423.

Chen CT, Hwang LL, Chang JK & Dun NJ (2000). Pressor effects of orexins injected intracisternally and to rostral ventrolateral medulla of anesthetized rats. *Am J Physiol* **278**, R692–697.

Coote JH (1988). The organisation of cardiovascular neurons in the spinal cord. *Rev Physiol Biochem Pharmacol* **110**, 147–285.

Date Y, Mondal MS, Matsukura S & Nakazato M (2000). Distribution of orexin-A and orexin-B (hypocretins) in the rat spinal cord. *Neurosci Lett* **288**, 87–90.

de Lecea L, Kilduff TS, Peyron C, Gao X, Foye PE, Danielson PE, Fukuhara C, Battenberg EL, Gautvik VT, Bartlett FS 2nd, Frankel WN, van den Pol AN, Bloom FE, Gautvik KM & Sutcliffe JG (1998). The hypocretins, hypothalamus-specific peptides with neuroexcitatory activity. *Proc Natl Acad Sci U S A* **95**, 322–327.

Dixon AK, Richardson PJ, Lee K, Carter N & Freeman TC (1998). Expression profiling of single cells using 3 prime end amplification (TPEA) PCR. *Nucleic Acids Res* **26**, 4426–4431.

Gibson IC & Logan SD (1995). Effects of muscarinic receptor stimulation of sympathetic preganglionic neurones of neonatal rat spinal cord *in vitro*. *Neuropharmacology* **34**, 309–318.

Greco MA & Shiromani PJ (2001). Hypocretin receptor protein and mRNA expression in the dorsolateral pons of rats. *Brain Res Mol Brain Res* **88**, 176–182.

Hagan JJ, Leslie RA, Patel S, Evans ML, Wattam TA, Holmes S, Benham CD, Taylor SG, Routledge C, Hemmati P, Munton RP, Ashmeade TE, Shah AS, Hatcher JP, Hatcher PD, Jones DNC, Smith MI, Piper DC, Hunter AJ, Porter RA & Upton N(1999). Orexin A activates locus coeruleus cell firing and increases arousal in the rat. *Proc Natl Acad Sci U S A* **96**, 10911–10916.

Horvath TL, Peyron C, Diano S, Ivanov A, Aston-Jones G, Kilduff TS & van den Pol AN (1999) Hypocretin (Orexin) activation and synaptic innervation of the locus coeruleus noradrenergic system. *J Comp Neurol* **415**, 145–159.

Ivanov A & Aston-Jones G (2000). Hypocretin/orexin depolarizes and decreases potassium conductance in locus coeruleus neurons. *Neuroreport* **11**, 1755–1758.

LeDoux JE (1995). Emotion – clues from the brain. *Annu Rev Psychol* **46**, 209–235.

Lee K, Dixon AK, Richardson PJ & Pinnock RD (1999). Glucose-receptive neurones in the rat ventromedial hypothalamus express K-ATP channels composed of Kir6.1 and SUR1 subunits. *J Physiol* **515**, 439–452.

Lin S & Huang XF (1999). Altered hypothalamic c-Fos-like immunoreactivity in diet-induced obese mice. *Brain Res Bull* **49**, 215–219.

Logan SD, Pickering AE, Gibson IC, Nolan MF & Spanswick D (1996). Electrotonic coupling between rat sympathetic preganglionic neurones *in vitro*. *J Physiol* **495**, 491–502.

Matsumura K, Tsuchihashi T & Abe I (2001). Central orexin-A augments sympathoadrenal outflow in conscious rabbits. *Hypertension* **37**, 1382–1387.

Nolan MF & Logan SD (1998). Metabotropic glutamate receptor-mediated excitation and inhibition of sympathetic preganglionic neurones. *Neuropharmacology* **37**, 13–24.

Nolan MF, Logan SD & Spanswick D (1999). Electrophysiological properties of electrical synapses between rat sympathetic preganglionic neurones *in vitro*. *J Physiol* **519**, 753–764.

Pickering AE, Spanswick D & Logan SD (1991). Whole-cell recordings from sympathetic preganglionic neurons in rat spinal cord slices. *Neurosci Lett* **130**, 237–242.

Pickering AE, Spanswick D & Logan SD (1994). 5-HT-induced depolarisation and membrane potential oscillations in rat sympathetic preganglionic neurons *in vitro*. *J Physiol* **480**, 109–121.

Sakurai T, Amemiya A, Ishii M, Matsuzaki I, Chemelli RM, Tanaka H, Williams SC, Richardson JA, Kozlowski GP, Wilson S, Arch JrS, Buckingham RE, Haynes AC, Carr SA, Annan RS, McNulty DE, Liu WS, Terrett JA, Elshourbagy NA, Bergsma DJ & Yanagisawa M (1998). Orexins and orexin receptors, a family of hypothalamic neuropeptides and G protein-coupled receptors that regulate feeding behavior. *Cell* **92**, 573–585.

Samson WK, Gosnell B, Chang JK, Resch ZT & Murphy TC (1999). Cardiovascular regulatory actions of the hypocretins in brain. *Brain Res* **831**, 248–253.

Shirasaka T, Nakazato M, Matsukura S, Takasaki M & Kannan H (1999). Sympathetic and cardiovascular actions of orexins in conscious rats. *Am J Physiol* **277**, R1780–1785.

Smart D, Jerman JC, Brough SJ, Neville WA, Jewitt F & Porter RA (2000). The hypocretins are weak agonists at recombinant human orexin-1 and orexin-2 receptors. *Br J Pharmacol* **129**, 1289–1291.

Smart D, Sabido-David C, Brough SJ, Jewitt F, Johns A, Porter RA & Jerman JC (2001). SB-334867-A, the first selective orexin-1 receptor antagonist. *Br J Pharmacol* **132**, 1179–1182.

Smith OA, Devito JL & Astley CA (1990). Neurons controlling cardiovascular responses to emotion are located in lateral hypothalamus-perifornical region. *Am J Physiol* **259**, R943–954.

Soffin EM, Evans ML, Gill CH, Harries MH, Benham CD & Davies CH (2002). SB-334867-A antagonises orexin mediated excitation in the locus coeruleus. *Neuropharmacology* **42**, 127–133.

Spanswick D & Logan SD (1990). Spontaneous rhythmic activity in the intermediolateral cell nucleus of the neonatal rat thoracolumbar spinal cord *in vitro*. *Neurosci* **39**, 395–403.

Spanswick D, Pickering AE, Gibson IC & Logan SD (1995). Excitation of sympathetic preganglionic neurones via metabotropic excitatory amino acid receptors. *Neurosci* **68**, 1247–1261.

Strack AM & Loewy AD (1990). Pseuorabies virus, a highly specific transneuronal cell body marker in the sympathetic nervous system. *J Neurosci* **10**, 2139–2147.

Strack AM, Sawyer WB, Hughes JH, Platt KB & Loewy AD (1989). A general pattern of CNS innervation of the sympathetic outflow demonstrated by transneuronal pseudorabies viral infections. *Brain Res* **491**, 156–162.

Stuart GJ, Dodt HU & Sakmann B (1993). Patch-clamp recordings from the soma and dendrites of neurons in brain-slices using infrared video microscopy. *Pflugers Arch* **423**, 511–518.

Sunter D, Morgan I, Edwards MB, Dakin, CL, Murphy KG, Gardiner J, Taheri S, Rayes E & Bloom SR (2001). Orexins, effects on behavior and localisation of orexin receptor 2 messenger ribonucleic acid in the rat brainstem. *Brain Research* **907**, 27–34.

Surmeier DJ, Song W-J & Yan Z (1996). Coordinated expression of dopamine receptors in neostriatal medium spiny neurons. *J Neurosci* **16**, 6579–6591.

Travagli RA, Dunwiddie TV & Williams JT (1995). Opioid inhibition in the locus coeruleus. *J Neurophysiol* **74**, 519–528.

van den Pol AN (1999). Hypothalamic hypocretin (orexin), robust innervation of the spinal cord. *J Neurosci* **19**, 3171–3182.

van den Pol AN, Gao XB, Obrietan K, Kilduff TS & Belousov AB (1998). Presynaptic and postsynaptic actions and modulation of neuroendocrine neurons by a new hypothalamic peptide, Hypocretin/Orexin. *J Neurosci* **18**, 7962–7971.

van den Pol AN, Ghosh PK, Liu R, Li Y, Aghajanian GK & Gao X-B (2002) Hypocretin (Orexin) enhances neuron activity and cell synchrony in developing mouse GFP-expressing locus coeruleus. *J Physiol* **541**, 169–185.

van den Top M, Lee K, Richardson PJ, Spanswick D & Nolan MF (2000). Orexin depolarizes rat sympathetic preganglionic neurones *in vitro*. *J Physiol* **528.P**, 107–108*P*.

van den Top M, Buijs RM, Ruijter JM, Delagrange P, Spanswick D & Hermes MLHJ (2001). Melatonin generates an outward potassium current in rat suprachiasmatic nucleus neurones *in vitro* independent of their circadian rhythm. *Neurosci* **107**, 99–108.

Acknowledgements

This work was supported by The Wellcome Trust, the BHF and The William Ramsay Henderson Trust.